Preliminary characterization of an optical current sensor for HVDC networks

G. Fusiek and P. Niewczas
Department of Electronic and Electrical Engineering, University of Strathclyde, Glasgow, UK
g.fusiek@strath.ac.uk

***Abstract*— An optical current sensor (OCS) for distributed current measurements on high-voltage direct current (HVDC) networks is presented in this paper. The sensor prototype, comprising a piezoelectric transducer and a fiber Bragg grating (FBG) as a principal optical strain sensing element, is evaluated through laboratory testing and its performance is assessed within the context of the accuracy requirements specified by the relevant industry standards. It is demonstrated that the device has the potential to meet the requirements of the accuracy class 1 specified by the IEC 61869-14 standard.**

Keywords—Fiber Bragg grating, optical current sensor, optical voltage sensor, power system instrumentation, HVDC network

I. Introduction

HVDC networks require high current and voltage monitoring over extended distances with fast reaction times from the protection systems [1]-[4]. Fast response, an order of magnitude faster than for AC equivalents, is mandatory to meet disconnection times better than 30 ms [2]. Distributed voltage and current metering and wide-area network protection can be realized using novel photonic sensor systems that facilitate improved network visibility and ensure fast reaction while remaining cost competitive with current technology.

We previously proposed optical voltage and current sensors for protection applications in AC networks and evaluated their performance according to the relevant industry standards [5]-[7]. In this paper, we focus on the design and preliminary evaluation of a prototype OCS demonstrating its potential to provide current measurements in HVDC networks. Selection of suitable components for the sensors construction, their dimensions, FBG attachment methods and its packaging are proposed in order to ensure it complies with the metering and protection classes and safety requirements of HVDC networks. The device performance is compared to the requirements stated in IEC 61869-14 for DC Current Transformers (DCCT) as the most appropriate standard [8].

II. Optical current sensor

A. Sensor concept

The concept of the proposed HVDC optical current sensor is shown in Fig. 1. A standard shunt resistor with a nominal output voltage of 100 mV is used to convert the line DC current into voltage. Voltage across the shunt is amplified by a low power precision amplifier to drive an optical voltage sensor combining photonic and piezoelectric technologies. The amplifier is powered from an energy harvester connected to the shunt resistor. Thus, no additional power supply provision is required for the amplifier at the sensor location.

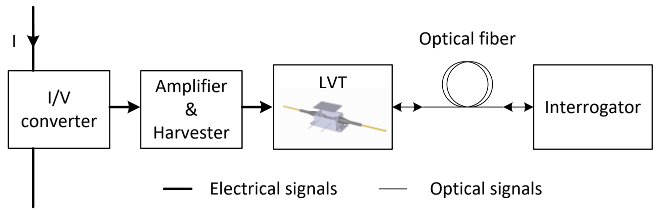

Fig. 1. HVDC sensor concept.

B. Low voltage transducer

A low voltage transducer (LVT) comprises a low-voltage piezoelectric multilayer stack and a bonded fiber Bragg grating (FBG) sensor [6]. The transducer is housed in an industry standard, hermetically sealed butterfly package (see Fig. 2). Voltage input to the piezoelectric stack is through the Kovar pins. Strain proportional to the input voltage is imparted to the FBG by the piezoelectric stack. In response, the wavelength reflected by the FBG shifts, due to the change in period of the grating. By tracking the peak reflected wavelength using an FBG interrogation system (see Fig. 1), the voltage input can be reconstructed. When the voltage source is a shunt resistor, this optical strain signal can be used to reconstruct the primary current [6].

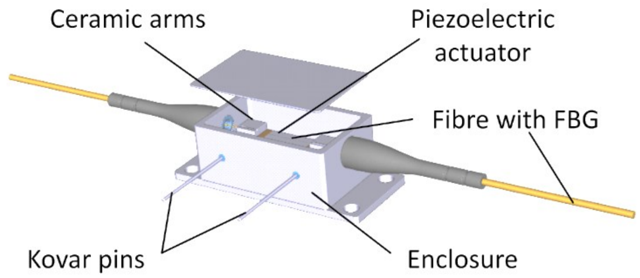

Fig. 2. Low voltage transducer.

In the proposed design, an FBG sensor was suspended between two ceramic arms attached to a rectangular block of PICMA® stack, having dimensions 3×3×9 mm. The FBG was attached to the arms with a UV epoxy [6], [7]. To enable DC measurements and temperature compensation capabilities, the sensor was equipped with an additional temperature FBG [7].

As specified by the manufacturer [9], the piezoelectric component used in the LVT construction has an operating

Research presented in this paper was supported by the Innovate UK (project number 102594) and the UK Engineering and Physical Sciences Research Council (grant reference EP/P510300/1).

voltage range from -30 V to 120 V. It has a resonant frequency of 135 kHz and can reach its full displacement in approximately 2.5 μs after the driving voltage change. The LVT nominal voltage was 2 V.

C. *Precision amplifier*

To ensure an appropriate strain-to-voltage response of the LVT, a sufficiently high voltage needs to be provided across the component. Since the nominal voltage of the sensor is 2 V, the signal from the shunt resistor requires amplification which is realized by means of a precision CMOS rail-to-rail op-amp, TLC4502 (Texas Instruments) [10]. It is used in a non-inverting configuration with a voltage follower connected to its output to match the LVT impedance. The op-amp requires low power supply, and hence, it can be powered from an energy harvester. Its maximum supply voltage is 6 V and the output current that the unit can provide is up to 100 mA. This is far more than required for driving the LVT.

D. *Energy harvester*

The energy harvester employed in the design utilises a highly integrated DC/DC voltage step-up converter, LTC3108 (Linear Technologies) [11]. The unit operates from as low input voltage as 20 mV and is capable of providing a selectable output voltage of 2.35 V, 3.3 V, 4.1 V or 5 V at loads of a few mA. The harvester circuitry is equipped with four 1 F capacitors to store energy for longer power outages. Due to the used high value capacitors, the charging time is relatively long as shown in Section IV.

III. ACCURACY CLASS REQUIREMENTS

The permissible amplitude errors at various points of the sensor measurement range for DC current transformers (DCCT) are presented in TABLE I based on IEC 61869-14 [8].

TABLE I. LIMITS OF RATIO ERROR FOR DCCT (61869-14)

Accuracy class	Ratio error ± %				
	at current (% of rated)				
	5	20	100	K_{pcr}	K_{ALF}
0,1	1	0,25	0,1	0,1	1
0,2	2	0,5	0,2	0,2	2
0,5	3,5	1	0,5	0,5	5
1	5	2	1	1	10

The K_{AFL} and K_{pcr} values, specified in TABLE I, are the accuracy limit factor and the extended primary current factor, respectively. The standard values of K_{AFL} are 5, 10, 20, 30 and 40 [8].

IV. EXPERIMENTAL RESULTS

A. *Experimental setup*

In order to evaluate the sensor performance, a series of tests was performed at room temperature and at different input current values. The experimental setup is shown in Fig. 3.

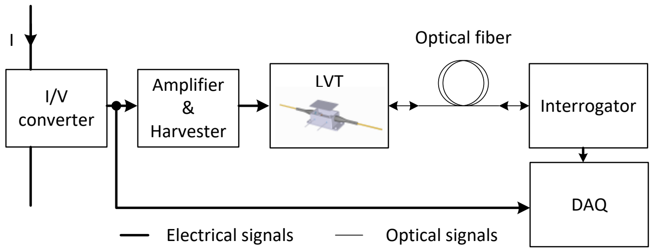

Fig. 3. Experimental setup for sensor characterization.

A regulated DC power supply and a resistive voltage divider were used to provide the required current in the tested circuit. The voltage across the shunt resistor was monitored by the optical sensor after amplification. During the tests, the optical sensor was monitored using a commercial interrogator connected to a PC equipped with a multifunction data acquisition (DAQ) card that was used to acquire reference voltage signals from the shunt. The data acquisition and sensor interrogation rates were set to 5 kS/s and were synchronized with each other. A dedicated program created in LabVIEW was used to process the raw sensor response in the form of instantaneous FBG wavelengths and the acquired reference voltage signals, and to calculate the measurement errors.

B. *Sensor components characterization*

Prior to the sensor accuracy tests the input-output characterization of the amplifier and the OCS was performed. As can be seen from Fig. 4, a gain of 21 V/V was achieved for the amplifier circuit. The harvester charging time from 0 to 5 V was 14.5 h for the input voltage of 60 mV and 1.25 h for 120 mV, respectively.

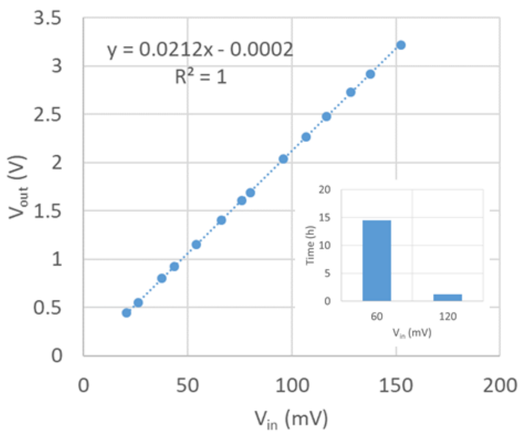

Fig. 4. Input-Output characteristic of the amplifier powered from the harvester. The inset shows charging times of the harvester as a function of the input voltage.

The relationship between the FBG peak wavelength and the reference voltage for the sensor is shown in Fig. 5. Each point on the characteristic was averaged from 5000 samples. The characteristic was then inverted and used to calibrate the sensor.

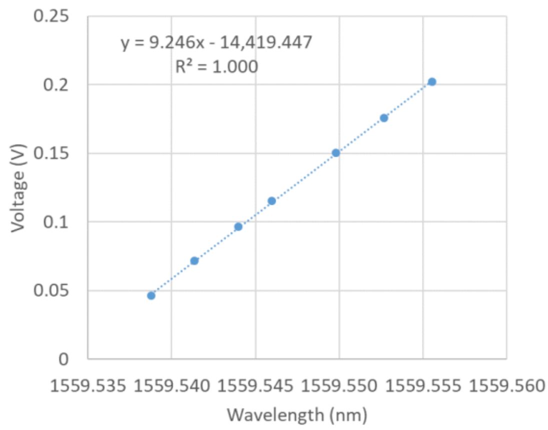

Fig. 5. Inverted sensor characteristic as a function of voltage across the shunt.

C. Measurement errors

The measurement error between the measured and reference voltage across the shunt was calculated according to the following equation: $\varepsilon(\%) = 100\cdot(V_{ref} - V_{rec})/V_{ref}$, where V_{ref} is the value of the reference voltage and V_{rec} is the value of the reconstructed voltage. The voltage characterization was performed on the sensor in laboratory conditions and according to IEC 61869-14. To assess the sensor suitability for measuring purposes, the acquired voltage levels having amplitudes between 50 % and 200 % of the device rated voltage were applied. The measurement errors are well below 1 % of the OCS nominal rating as shown in Fig. 6.

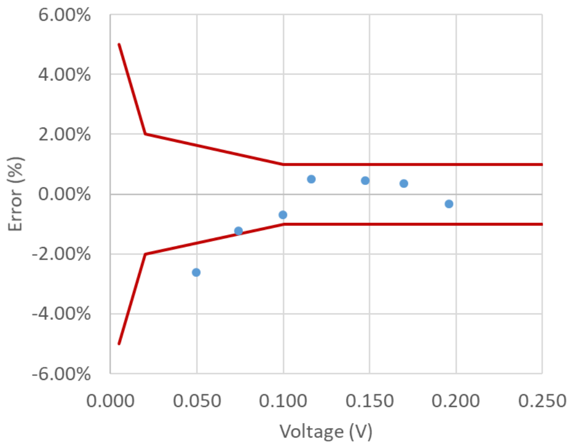

Fig. 6. Optical sensor measurement errors.

It should be noted that due to the interrogator available for the experiments, the measurement errors are relatively high, especially at lower voltages below 75 % of the sensor nominal voltage. This is because of the interrogator having a poor spectral resolution of 2 pm while the maximum signal on the sensor was approximately 20 pm. It is expected that the error can be reduced when the optical interrogator having a better spectral resolution and accuracy is used.

V. Conclusions

In this paper, the design and construction of an optical current sensor (OCS) for distributed current measurement on High-Voltage Direct Current (HVDC) networks has been presented. The sensor performance was evaluated experimentally in laboratory conditions according to the IEC 61869-14 standard. The preliminary results indicate that the measurement errors are well below 1 % of the sensor nominal rating. The errors can be reduced when the optical interrogator having a better spectral resolution and accuracy is used.

Acknowledgment

The authors thank Dr Philip Orr and Dr Neil Gordon of Synaptec for providing an LVT for the HVDC OCS prototype construction and testing.

References

[1] S. Pirooz Azad and D. Van Hertem, “A Fast Local Bus Current-Based Primary Relaying Algorithm for HVDC Grids,” IEEE Trans. Power Deliv., vol. 32, no. 1, pp. 193–202, Feb. 2017.

[2] M. Hajian, D. Jovcic, and B. Wu, “Evaluation of Semiconductor Based Methods for Fault Isolation on High Voltage DC Grids,” IEEE Trans. Smart Grid, vol. 4, no. 2, 2013.

[3] M. K. Bucher and C. M. Franck, “Fault Current Interruption in Multiterminal HVDC Networks,” IEEE Trans. Power Deliv., vol. 31, no. 1, pp. 87–95, Feb. 2016.

[4] M. K. Bucher and C. M. Franck, “Analytic Approximation of Fault Current Contribution From AC Networks to MTDC Networks During Pole-to-Ground Faults,” IEEE Trans. Power Deliv., vol. 31, no. 1, pp. 20–27, Feb. 2016.

[5] P. Orr, G. Fusiek, P. Niewczas, C. Booth, A. Dyśko, F. Kawano, T. Nishida, P. Beaumont, “Distributed Photonic Instrumentation for Power System Protection and Control” IEEE Transactions on Instrumentation and Measurement journal, 64(1) 2015

[6] J. Nelson, G. Fusiek, L. Clayburn, P. Niewczas, C. Booth, P. Orr, N. Gordon, “Development and testing of optically-interrogated current sensors”, AMPS 2016

[7] G. Fusiek, J. Nelson, P. Niewczas, J. Havunen, E. P. Suomalainen and J. Hällström, "Optical voltage sensor for MV networks," 2017 IEEE SENSORS, Glasgow, 2017, pp. 1-3.

[8] IEC 61869, “Instrument transformers – Part 14: Specific Requirements for DC Current Transformers,” Draft (2014)

[9] Physik Instrumente Ltd website, available at: http://www.piceramic.com/index.php

[10] Texas Instruments, “TLC4501, TLC4501A, TLC4502, TLC4502A Family of self-calibrating (self-cal) precision cmos rail-to-rail output operational amplifiers”, datasheet.

[11] Linear Technology, “LTC3108 - Ultralow Voltage Step-Up Converter and Power Manager.”, datasheet.